

# Propagation effects of Lorentz violation in gravitational waves

A. A. Araújo Filho,<sup>1,2,3,\*</sup> N. Heidari,<sup>2,3,4,†</sup> and Iarley P. Lobo<sup>2,5,‡</sup>

<sup>1</sup>*Departamento de Física, Universidade Federal da Paraíba,  
Caixa Postal 5008, 58051-970, João Pessoa, Paraíba, Brazil.*

<sup>2</sup>*Departamento de Física, Universidade Federal de Campina Grande Caixa Postal 10071,  
58429-900 Campina Grande, Paraíba, Brazil.*

<sup>3</sup>*Center for Theoretical Physics, Khazar University,  
41 Mehseti Street, Baku, AZ-1096, Azerbaijan.*

<sup>4</sup>*School of Physics, Damghan University, Damghan, 3671641167, Iran.*

<sup>5</sup>*Department of Chemistry and Physics, Federal University of Paraíba,  
Rodovia BR 079 - km 12, 58397-000 Areia-PB, Brazil.*

(Dated: February 24, 2026)

## Abstract

We investigate the propagation of gravitational waves in the presence of Lorentz- and diffeomorphism-violating operators within the linearized gravitational sector of the Standard Model Extension. Focusing on isotropic contributions, we analyze the combined effects of the nondispersive CPT-even dimension-four coefficient  $\overset{\circ}{k}_{(I)}^{(4)}$  and the CPT-odd dimension-five coefficient  $\overset{\circ}{k}_{(V)}^{(5)}$  on tensorial gravitational radiation. The modified dispersion relation induces both a rescaling of the propagation speed and helicity-dependent dispersive corrections, leading to birefringence and polarization mixing without introducing additional propagating degrees of freedom. We derive the retarded Green function associated with the modified wave operator and obtain explicit expressions for the gravitational waveform generated by matter sources. As a concrete application, we examine a binary black hole system and show how Lorentz violation alters the observed strain through shifted retarded times, amplitude rescaling, and higher derivative corrections to the quadrupole formula. The CPT-odd term produces characteristic attenuation and distortions in the waveform, which can be interpreted as energy exchange between the gravitational wave and the Lorentz-violating background rather than a violation of energy conservation. Using published LIGO-Virgo-KAGRA propagation tests and polarization consistency arguments, we translate current observational constraints into bounds on  $\overset{\circ}{k}_{(I)}^{(4)}$  and  $\overset{\circ}{k}_{(V)}^{(5)}$ .

---

\*Electronic address: [dilto@fisica.ufc.br](mailto:dilto@fisica.ufc.br)

†Electronic address: [heidari.n@gmail.com](mailto:heidari.n@gmail.com)

‡Electronic address: [lobofisica@gmail.com](mailto:lobofisica@gmail.com)

## Contents

<b>I. Introduction</b>	2
<b>II. Theoretical framework</b>	5
<b>III. Polarization structure of Lorentz–violating gravitational waves</b>	9
<b>IV. Gravitational wave emission from matter sources</b>	12
A. Application with a binary black hole system	15
<b>V. Bounds from LVK (Virgo/KAGRA-including catalogs) data</b>	20
A. Bound on the nondispersive coefficient $\mathring{k}_{(I)}^{(4)}$	22
B. Bounds on the CPT–odd $d = 5$ coefficient $\mathring{k}_{(V)}^{(5)}$	22
1. Translation from LVK parameterized dispersion tests	22
2. Birefringent phase accumulation	23
3. Strain–based effects	24
<b>VI. Conclusion</b>	26
<b>VII. Acknowledgments</b>	27
<b>VIII. Data Availability Statement</b>	28
<b>References</b>	28

## I. INTRODUCTION

General Relativity has established itself as the prevailing geometric framework for gravitational interactions, having undergone extensive scrutiny across a wide range of physical regimes. Its predictions have been confronted with high–precision measurements in laboratory experiments, solar–system tests, binary pulsars, gravitational–wave observations, and cosmological probes, consistently showing remarkable agreement with observational data [1–10]. Despite this empirical success, the theory does not constitute a complete description of gravitation. Several conceptual and theoretical obstacles remain unresolved within the classical formulation. At short distances, the occurrence of spacetime singularities signals a breakdown of the theory, while attempts to embed gravity into a consistent quantum framework encounter persistent difficulties.

On the other hand, on cosmological and galactic scales, the dynamics inferred from observations require additional ingredients—typically modeled as dark matter and dark energy—that do

not arise naturally from the Einstein equations themselves. These shortcomings suggest that the classical picture may represent only an effective description of a more fundamental gravitational theory. Such considerations have stimulated the development of alternative frameworks that extend or modify General Relativity. A number of these proposals are rooted in ideas from quantum gravity, including string-inspired constructions [11, 12], loop-based quantization schemes [13], and scenarios involving extra dimensions or brane embeddings [14]. A common feature shared by many of these approaches is a departure from one of the foundational assumptions of General Relativity: the exact and universal validity of Lorentz invariance and diffeomorphism symmetry.

An effective field theory perspective offers a natural arena for investigating potential violations of Lorentz invariance and diffeomorphism symmetry in gravitational physics. Within this approach, the Standard Model Extension (SME) was introduced as a comprehensive parametrization scheme designed to capture symmetry-breaking effects without committing to a specific microscopic theory [15, 16]. The construction of the SME does not rely on altering the geometric foundations of spacetime. Instead, it augments the action by systematically including all operators compatible with observer covariance that violate local Lorentz and diffeomorphism symmetries, classified according to their mass dimension and tensorial structure.

Over the past decades, this framework has played a central role in empirical searches for Lorentz violation, particularly in the nongravitational sector, where it has supported an extensive program of experimental and observational tests. The resulting bounds span a wide range of physical systems and energy scales. Once gravitational interactions are incorporated, the SME provides a unified language for analyzing precision measurements drawn from diverse observational settings. These include lunar laser ranging experiments [17, 18], atom-interferometry tests [19], studies of ultra-high-energy cosmic rays [20], pulsar-timing data [21–26], analyses of planetary ephemerides [27], and measurements performed with superconducting gravimeters [28]. In the majority of these investigations, observable effects arise predominantly through modified couplings between gravitational fields and matter degrees of freedom [29].

An alternative viewpoint is obtained by isolating the purely gravitational sector and examining its intrinsic dynamics. In this setting, Lorentz- and diffeomorphism-violating contributions are probed directly through their impact on the propagation of gravitational disturbances. Adopting a linearized description of the metric, gravitational waves provide a clean and sensitive channel for testing departures from standard relativistic behavior, independent of matter couplings [30–32].

In a weak-field description where gravity is expanded about a Minkowski background, possible violations of Lorentz symmetry enter through additional terms in the quadratic action for metric perturbations. These corrections are naturally classified within an effective field-theory expansion

by their mass dimension  $d$ . A further distinction emerges once their behavior under linearized coordinate transformations is taken into account. Specifically, the transformation  $h_{\mu\nu} \rightarrow h_{\mu\nu} + \partial_\mu \xi_\nu + \partial_\nu \xi_\mu$ , with  $h_{\mu\nu}$  representing small deviations from flat spacetime and  $\xi_\mu$  an arbitrary infinitesimal vector field, provides the criterion for identifying whether a given operator preserves or violates diffeomorphism symmetry at the linearized level.

Imposing invariance under this gauge transformation severely restricts the allowed operator content. In particular, Lorentz-violating terms that remain compatible with linearized diffeomorphism symmetry first appear at mass dimension  $d \geq 4$  [31, 33]. The consequences of such higher-dimensional operators for gravitational wave propagation, together with the corresponding phenomenological constraints, have been analyzed extensively in the literature [31, 33–42].

If the requirement of diffeomorphism invariance is instead relaxed in the linearized theory, the operator spectrum broadens substantially. In this case, Lorentz-violating contributions with lower mass dimension become admissible, including terms with  $d = 2$  and  $d = 3$  [31]. Such operators introduce qualitatively different modifications to the dynamics of metric perturbations and open additional possibilities for departures from standard relativistic propagation.

The systematic construction of Lorentz-violating contributions to the quadratic action for metric perturbations has been carried out in a comprehensive manner in Ref. [31]. That analysis identifies all admissible operators within the linearized gravitational sector, encompassing both terms that remain compatible with infinitesimal coordinate invariance and those that explicitly violate it. Once such operators are introduced, the propagation of gravitational waves departs from the standard relativistic picture in a generic way. Modifications typically appear in the form of anisotropic propagation, helicity-dependent phase velocities, and dispersive time delays, each of which can be encoded directly in the waveform morphology.

When linearized diffeomorphism symmetry is retained, the resulting corrections to gravitational wave dynamics admit a particularly transparent formulation. In this case, the altered propagation laws and their observational consequences have been derived explicitly in Ref. [37]. These results provide a direct bridge to data analysis, allowing the Lorentz-violating coefficients of the gravitational SME to be constrained through Bayesian inference applied to gravitational wave observations. A related but conceptually distinct approach has been developed using a parametrized framework tailored to symmetry-breaking effects in gravitational wave propagation [36]. Rather than starting from a specific operator basis, this method characterizes deviations at the level of effective propagation parameters. This formalism has been employed to investigate possible Lorentz-violating features in the primordial gravitational wave background, as explored in Ref. [43].

In this work, we build on and extend the analysis presented in Ref. [44] (also based on the

analysis of Ref. [45]), where gravitational wave propagation was examined in the presence of the CPT–even coefficient  $\overset{\circ}{k}_{(I)}^{(4)}$  alone. Here, on the other hand, we generalize that framework by incorporating additional Lorentz– and diffeomorphism–violating effects within the linearized gravitational sector of the Standard Model Extension. In this manner, focusing on isotropic contributions, we investigate the combined influence of the CPT–even dimension four coefficient  $\overset{\circ}{k}_{(I)}^{(4)}$  and the CPT–odd dimension five coefficient  $\overset{\circ}{k}_{(V)}^{(5)}$  on tensor gravitational waves. The modified dispersion relation leads to a rescaling of the propagation speed together with helicity–dependent dispersive corrections, giving rise to birefringence and polarization mixing without introducing extra propagating degrees of freedom. We derive the corresponding retarded Green function and obtain explicit expressions for the gravitational waveforms generated by matter sources. As a concrete application, we consider a binary black hole system and demonstrate how Lorentz violation alters the observed strain through shifts in the retarded time, amplitude rescaling, and higher–derivative corrections to the quadrupole formula. The CPT–odd term produces characteristic attenuation and waveform distortions, which can be interpreted as energy exchange with the Lorentz–violating background rather than a breakdown of energy conservation. Finally, using published LIGO–Virgo–KAGRA results, we translate current propagation and polarization constraints into bounds on  $\overset{\circ}{k}_{(I)}^{(4)}$  and  $\overset{\circ}{k}_{(V)}^{(5)}$ .

## II. THEORETICAL FRAMEWORK

We begin by outlining the treatment of gravitational radiation within the linearized gravitational sector of the Standard Model Extension. In this setting, departures from exact Lorentz and diffeomorphism invariance are incorporated through additional operators that act directly on the tensor perturbations of the metric. These terms alter the propagation properties of gravitational waves, producing modified dispersion relations that deviate from the relativistic form. The formulation relies on the quadratic expansion of the gravitational action about flat spacetime, where the effects of symmetry breaking are encoded as corrections to the free graviton dynamics [33, 46]

$$\mathcal{L} = \frac{1}{4}\epsilon^{\mu\rho\alpha\kappa}\epsilon^{\nu\sigma\beta\lambda}\eta_{\kappa\lambda}h_{\mu\nu}\partial_\alpha\partial_\beta h_{\rho\sigma} + \frac{1}{4}h_{\mu\nu}\sum_{\mathcal{K},d}\hat{\mathcal{K}}^{(d)\mu\nu\rho\sigma}h_{\rho\sigma}.$$

To describe weak gravitational fields, the spacetime metric is expanded about a flat background as  $g_{\mu\nu} = \eta_{\mu\nu} + h_{\mu\nu}$ , with  $\eta_{\mu\nu}$  representing the Minkowski metric and  $h_{\mu\nu}$  the dynamical perturbation. Within this setup, the symbol  $\epsilon^{\mu\rho\alpha\kappa}$  denotes the fully antisymmetric Levi–Civita tensor. At quadratic order in  $h_{\mu\nu}$ , the action reduces to the familiar linearized Einstein–Hilbert form, governing the standard propagation of tensor modes. Deviations from this behavior arise through additional contributions that violate Lorentz and diffeomorphism symmetries. Such effects are in-

incorporated by means of differential operators  $\hat{\mathcal{K}}^{(d)\mu\nu\rho\sigma}$ , which are built from constant background tensors contracted with spacetime derivatives and organized according to their mass dimension  $\mathcal{K}^{(d)\mu\nu\rho\sigma\alpha_1\dots\alpha_{d-2}}$  with  $d - 2$  spacetime derivatives  $\partial_{\alpha_1} \dots \partial_{\alpha_{d-2}}$

$$\hat{\mathcal{K}}^{(d)\mu\nu\rho\sigma} = \mathcal{K}^{(d)\mu\nu\rho\sigma\alpha_1\alpha_2\dots\alpha_{d-2}} \partial_{\alpha_1} \partial_{\alpha_2} \dots \partial_{\alpha_{d-2}}. \quad (1)$$

The coefficients  $\mathcal{K}^{(d)\mu\nu\rho\sigma\alpha_1\dots\alpha_{d-2}}$  are assigned mass dimension  $4 - d$  and are assumed to represent small, fixed background quantities on the spacetime scales relevant for gravitational wave propagation. These tensors enter the linearized dynamics only through specific index structures of the associated differential operators  $\hat{\mathcal{K}}^{(d)\mu\nu\rho\sigma}$ . In particular, nontrivial contributions arise when the operator fails to exhibit symmetry under the interchange of the index pairs  $(\mu\nu)$  and  $(\rho\sigma)$ . This condition can be expressed as  $K^{(d)(\mu\nu)(\rho\sigma)} \neq \pm K^{(d)(\rho\sigma)(\mu\nu)}$ , where the choice of the plus or minus sign is determined by whether the operator dimension  $d$  is odd or even, respectively [33, 46]

$$\hat{\mathcal{K}}^{(d)\mu\nu\rho\sigma} = \tilde{\hat{s}}^{(d)\mu\rho\nu\sigma} + \tilde{\hat{q}}^{(d)\mu\rho\nu\sigma} + \tilde{\hat{k}}^{(d)\mu\rho\nu\sigma}. \quad (2)$$

Based on their index symmetries, Lorentz-violating operators appearing in the quadratic gravitational action can be grouped into a small number of distinct categories. This classification is determined by the transformation properties of their tensor indices under permutations. One subset consists of operators  $\tilde{\hat{s}}^{(d)\mu\rho\nu\sigma}$  that are antisymmetric within both index pairs  $(\mu\rho)$  and  $(\nu\sigma)$ . A second subset, labeled  $\tilde{\hat{q}}^{(d)\mu\rho\nu\sigma}$ , exhibits mixed symmetry, being antisymmetric in  $(\mu\rho)$  while remaining symmetric in  $(\nu\sigma)$ . The final subset, denoted  $\tilde{\hat{k}}^{(d)\mu\rho\nu\sigma}$ , is constructed to be completely symmetric under all index interchanges. Each of these operator families can be further resolved into irreducible tensor components, a step that clarifies the distinct ways in which they modify the propagation of gravitational waves. Carrying out this decomposition leads to a total of fourteen independent operator classes, as cataloged in Table I of Refs. [33, 46].

Within this classification, the  $\tilde{\hat{s}}$ -sector plays a special role. The operators  $\tilde{\hat{s}}^{(d)\mu\rho\nu\sigma}$  are CPT-even, remaining unchanged under the combined action of charge conjugation, parity, and time reversal. Their tensorial structure allows them to be expressed in terms of three separate irreducible contributions, which can be analyzed independently in the context of gravitational wave dynamics

$$\tilde{\hat{s}}^{(d)\mu\rho\nu\sigma} = \tilde{\hat{s}}^{(d,0)\mu\rho\nu\sigma} + \tilde{\hat{s}}^{(d,1)\mu\rho\nu\sigma} + \tilde{\hat{s}}^{(d,2)\mu\rho\nu\sigma}, \quad (3)$$

with we have

$$\begin{aligned} \tilde{\hat{s}}^{(d,0)\mu\rho\nu\sigma} &= s^{(d,0)\mu\rho\alpha_1\nu\sigma\alpha_2\alpha_3\dots\alpha_{d-2}} \partial_{\alpha_1} \dots \partial_{\alpha_{d-2}}, \\ \tilde{\hat{s}}^{(d,1)\mu\rho\nu\sigma} &= s^{(d,1)\mu\rho\nu\sigma\alpha_1\dots\alpha_{d-2}} \partial_{\alpha_1} \dots \partial_{\alpha_{d-2}}, \\ \tilde{\hat{s}}^{(d,2)\mu\rho\nu\sigma} &= s^{(d,2)\mu\rho\alpha_1\nu\sigma\alpha_2\alpha_3\dots\alpha_{d-2}} \partial_{\alpha_1} \dots \partial_{\alpha_{d-2}}. \end{aligned} \quad (4)$$

A different behavior characterizes the operators belonging to the  $\tilde{q}$  sector. The tensors  $\tilde{q}^{(d)\mu\rho\nu\sigma}$  are CPT–odd and consequently change sign under the simultaneous application of charge conjugation, parity, and time reversal. Owing to their mixed symmetry properties, these operators admit a decomposition into six mutually independent irreducible components, each contributing in a distinct manner to modifications of gravitational wave propagation

$$\tilde{q}^{(d)\mu\rho\nu\sigma} = \tilde{q}^{(d,0)\mu\rho\nu\sigma} + \tilde{q}^{(d,1)\mu\rho\nu\sigma} + \tilde{q}^{(d,2)\mu\rho\nu\sigma} + \tilde{q}^{(d,3)\mu\rho\nu\sigma} + \tilde{q}^{(d,4)\mu\rho\nu\sigma} + \tilde{q}^{(d,5)\mu\rho\nu\sigma}, \quad (5)$$

where

$$\begin{aligned} \tilde{q}^{(d,0)\mu\rho\nu\sigma} &= \tilde{q}^{(d,0)\mu\rho\alpha_1\nu\alpha_2\sigma\alpha_3\alpha_4\dots\alpha_{d-2}}\partial_{\alpha_1}\dots\partial_{\alpha_{d-2}}, \\ \tilde{q}^{(d,1)\mu\rho\nu\sigma} &= \tilde{q}^{(d,1)\mu\rho\nu\sigma\alpha_1\alpha_2\dots\alpha_{d-2}}\partial_{\alpha_1}\dots\partial_{\alpha_{d-2}}, \\ \tilde{q}^{(d,2)\mu\rho\nu\sigma} &= \tilde{q}^{(d,2)\mu\rho\nu\alpha_1\sigma\alpha_2\dots\alpha_{d-2}}\partial_{\alpha_1}\dots\partial_{\alpha_{d-2}}, \\ \tilde{q}^{(d,3)\mu\rho\nu\sigma} &= \tilde{q}^{(d,3)\mu\rho\alpha_1\nu\sigma\alpha_2\dots\alpha_{d-2}}\partial_{\alpha_1}\dots\partial_{\alpha_{d-2}}, \\ \tilde{q}^{(d,4)\mu\rho\nu\sigma} &= \tilde{q}^{(d,4)\mu\rho\nu\alpha_1\sigma\alpha_2\alpha_3\alpha_4\dots\alpha_{d-2}}\partial_{\alpha_1}\dots\partial_{\alpha_{d-2}}, \\ \tilde{q}^{(d,5)\mu\rho\nu\sigma} &= \tilde{q}^{(d,5)\mu\rho\alpha_1\nu\alpha_2\sigma\alpha_3\alpha_4\dots\alpha_{d-2}}\partial_{\alpha_1}\dots\partial_{\alpha_{d-2}}. \end{aligned} \quad (6)$$

It is worthy commenting that operators in the  $\tilde{k}$  sector are CPT–even and can be resolved into five independent irreducible components

$$\tilde{k}^{(d)\mu\nu\rho\sigma} = \tilde{k}^{(d,0)\mu\nu\rho\sigma} + \tilde{k}^{(d,1)\mu\nu\rho\sigma} + \tilde{k}^{(d,2)\mu\nu\rho\sigma} + \tilde{k}^{(d,3)\mu\nu\rho\sigma} + \tilde{k}^{(d,4)\mu\nu\rho\sigma},$$

in a such way that

$$\begin{aligned} \tilde{k}^{(d,0)\mu\nu\rho\sigma} &= \tilde{k}^{(d,0)\mu\alpha_1\nu\alpha_2\rho\alpha_3\sigma\alpha_4\alpha_5\dots\alpha_{d-2}}\partial_{\alpha_1}\dots\partial_{\alpha_{d-2}}, \\ \tilde{k}^{(d,1)\mu\nu\rho\sigma} &= \tilde{k}^{(d,1)\mu\nu\rho\sigma\alpha_1\dots\alpha_{d-2}}\partial_{\alpha_1}\dots\partial_{\alpha_{d-2}}, \\ \tilde{k}^{(d,2)\mu\nu\rho\sigma} &= \tilde{k}^{(d,2)\mu\alpha_1\nu\rho\sigma\alpha_1\alpha_2\dots\alpha_{d-2}}\partial_{\alpha_1}\dots\partial_{\alpha_{d-2}}, \\ \tilde{k}^{(d,3)\mu\nu\rho\sigma} &= \tilde{k}^{(d,3)\mu\alpha_1\nu\alpha_2\rho\sigma\alpha_3\alpha_5\dots\alpha_{d-2}}\partial_{\alpha_1}\dots\partial_{\alpha_{d-2}}, \\ \tilde{k}^{(d,4)\mu\nu\rho\sigma} &= \tilde{k}^{(d,4)\mu\alpha_1\nu\alpha_2\rho\alpha_3\sigma\alpha_4\alpha_5\dots\alpha_{d-2}}\partial_{\alpha_1}\dots\partial_{\alpha_{d-2}}. \end{aligned} \quad (7)$$

At the level of linearized gravitational dynamics, all possible Lorentz–violating effects can be parametrized by a finite set of coefficients. This construction leads to fourteen independent coefficient classes, whose defining symmetry properties and tensorial structures are summarized in Table I of Refs. [33, 46], as argued before. Taken together, these coefficients exhaust the space

of allowed modifications to graviton propagation at quadratic order and capture every observable deviation from the standard relativistic behavior of gravitational waves within this framework.

Requiring invariance under infinitesimal coordinate redefinitions imposes severe constraints on the form of these terms in the linearized theory. In particular, demanding that the quadratic action  $S \sim \int d^4x \mathcal{L}$  remain invariant under the gauge transformation  $h_{\mu\nu} \rightarrow h_{\mu\nu} + \partial_\mu \xi_\nu + \partial_\nu \xi_\mu$  leads to a nontrivial condition on the allowed operator structure. The Lorentz-violating operator must then obey the relation  $\hat{\mathcal{K}}^{(d)(\mu\nu)(\rho\sigma)} \partial_\nu = \pm \hat{\mathcal{K}}^{(d)(\rho\sigma)(\mu\nu)} \partial_\nu$ , where the sign depends on the operator dimension.

Enforcing this constraint drastically reduces the space of admissible operators. The general Lorentz-violating sector collapses into three distinct classes, conventionally labeled as  $\tilde{\hat{s}}^{(d,0)\mu\rho\nu\sigma}$ ,  $\tilde{\hat{q}}^{(d,0)\mu\rho\nu\sigma}$ , and  $\tilde{\hat{k}}^{(d,0)\mu\rho\nu\sigma}$  [33, 46]. An additional hierarchy follows from symmetry considerations: if linearized diffeomorphism invariance is preserved, Lorentz-violating effects are restricted to operators with mass dimension  $d \geq 4$ , whereas relaxing this requirement allows contributions already at  $d \geq 2$ .

The equations that determine the propagation of gravitational waves are obtained by extremizing the quadratic action  $S \sim \int d^4x \mathcal{L}$  with respect to the metric fluctuation  $h_{\mu\nu}$ . Substituting the Lagrangian density introduced in Eq. (1) and carrying out the functional variation yields

$$\frac{1}{2} \eta_{\rho\sigma} \epsilon^{\mu\rho\alpha\kappa} \epsilon^{\nu\sigma\beta\lambda} \partial_\alpha \partial_\beta h_{\kappa\lambda} - \delta M^{\mu\nu\rho\sigma} h_{\rho\sigma} = 0, \quad (8)$$

where the tensor operators take the form

$$\delta M^{\mu\nu\rho\sigma} = -\frac{1}{4} \left( \tilde{\hat{s}}^{\mu\rho\nu\sigma} + \tilde{\hat{s}}^{\mu\sigma\nu\rho} \right) - \frac{1}{2} \tilde{\hat{k}}^{\mu\nu\rho\sigma} - \frac{1}{8} \left( \tilde{\hat{q}}^{\mu\rho\nu\sigma} + \tilde{\hat{q}}^{\nu\rho\mu\sigma} + \tilde{\hat{q}}^{\mu\sigma\nu\rho} + \tilde{\hat{q}}^{\nu\sigma\mu\rho} \right). \quad (9)$$

so that

$$\tilde{\hat{s}}^{\mu\rho\nu\sigma} = \sum_d \tilde{\hat{s}}^{(d)\mu\rho\nu\sigma}, \quad (10)$$

$$\tilde{\hat{q}}^{\mu\rho\nu\sigma} = \sum_d \tilde{\hat{q}}^{(d)\mu\rho\nu\sigma}, \quad (11)$$

$$\tilde{\hat{k}}^{\mu\rho\nu\sigma} = \sum_d \tilde{\hat{k}}^{(d)\mu\rho\nu\sigma}. \quad (12)$$

In the framework of General Relativity, gravitational waves propagate through a highly constrained channel, being described solely by two transverse traceless tensor polarizations. This economy of degrees of freedom relies on the exact validity of Lorentz invariance and diffeomorphism symmetry. Once these symmetries are relaxed, the polarization content of metric perturbations need not remain limited to the tensor sector. In more general settings, additional scalar and vector excitations may become dynamical, extending the spectrum of gravitational wave polarizations beyond the standard picture. In linearized gravity with Lorentz-violating terms however,

such non-tensorial modes do not necessarily arise as independent sources. Instead, they can be activated through couplings to the tensor perturbations themselves, leading to indirect excitation mechanisms, as discussed in Refs. [34, 46]. In other words, the presence and relevance of these extra components depend sensitively on the structure of the symmetry-breaking operators.

From an observational standpoint, however, no deviations from the tensor-only polarization pattern have been detected so far. Analyses performed by the LIGO–Virgo–KAGRA Collaboration are fully compatible with the propagation of two tensor modes and show no statistically significant evidence for scalar or vector polarizations [47]. Moreover, even in scenarios where such modes exist, their contributions are expected to be strongly suppressed relative to the dominant tensor signal.

Guided by these experimental findings and aiming for a focused theoretical treatment, we restrict attention to the transverse traceless tensor sector in what follows. Any additional polarizations are assumed to be negligible, and the analysis proceeds in close analogy with Ref. [33], concentrating on how Lorentz- and diffeomorphism-violating operators modify the propagation of the two tensorial gravitational wave modes alone.

### III. POLARIZATION STRUCTURE OF LORENTZ-VIOLATING GRAVITATIONAL WAVES

For Lorentz-violating operators of mass dimension  $d = 4$ , the modified dispersion relation simplifies considerably, taking a compact form [33]

$$p^0 = \left(1 - \varsigma_0 \pm \sqrt{\varsigma_1^2 + \varsigma_2^2 + \varsigma_3^2}\right) |\vec{p}|. \quad (13)$$

In this expression,  $p^\mu = (p^0, \vec{p})$  represents the four-momentum of the gravitational wave. The quantities  $\varsigma_i$  collect all contributions associated with Lorentz violation and are constructed as momentum-dependent combinations of gauge-invariant operators entering the quadratic action for metric fluctuations. The detailed form of these functions can be found in Ref. [33]

$$\varsigma_0 = \frac{1}{4p^2} \left\{ -\tilde{s}^{\mu\nu}{}_{\mu\nu} + \frac{1}{2} \tilde{k}^{\mu\nu}{}_{\mu\nu} \right\}, \quad (14)$$

$$(\varsigma_1)^2 + (\varsigma_2)^2 = \frac{1}{8p^4} \left\{ \tilde{k}^{\mu\nu\rho\sigma} \tilde{k}_{\mu\nu\rho\sigma} - \tilde{k}^{\mu\rho}{}_{\nu\rho} \tilde{k}_{\mu\sigma}{}^{\nu\sigma} + \frac{1}{8} \tilde{k}^{\mu\nu}{}_{\mu\nu} \tilde{k}^{\rho\sigma}{}_{\rho\sigma} \right\}, \quad (15)$$

$$(\varsigma_3)^2 = \frac{1}{16p^4} \left\{ -\frac{1}{2} \tilde{q}^{\mu\rho\nu\sigma} \tilde{q}_{\mu\rho\nu\sigma} - \tilde{q}^{\mu\nu\rho\sigma} \tilde{q}_{\mu\rho\nu\sigma} + (\tilde{q}^{\mu\rho\nu}{}_{\rho} + \tilde{q}^{\nu\rho\mu}{}_{\rho}) \tilde{q}_{\mu\sigma\nu}{}^{\sigma} \right\}. \quad (16)$$

In momentum space, the Lorentz-violating operators are indicated by a hat and are obtained by substituting spacetime derivatives with factors of the wave four-momentum according to  $\partial_\mu \rightarrow ip_\mu$ .

The modified dispersion relation in Eq. (13) shows that Lorentz violation can affect gravitational wave propagation in three fundamentally distinct ways. One class of effects alters the angular response of the waves. If rotational symmetry is not preserved, the propagation becomes anisotropic, and the resulting behavior depends—within a fixed observer frame—on coefficients carrying explicit spatial indices. A separate modification concerns the dependence of the propagation speed on frequency. Such dispersion emerges whenever the effective operators depend on the wave momentum. In contrast, frequency-independent propagation is possible only in the special case of mass dimension  $d = 4$  operators, where the dynamics are controlled solely by the tensor  $\tilde{s}^{\mu\rho\nu\sigma}$ . Finally, Lorentz violation may induce a separation of polarization states during propagation. The existence of two distinct branches in the solutions of Eq. (13) reflects birefringence, signaling that different polarizations travel with different phase velocities. This phenomenon arises exclusively from the  $\tilde{q}^{\mu\rho\nu\sigma}$  and  $\tilde{k}^{\mu\nu\rho\sigma}$  sectors and therefore requires operators of mass dimension  $d > 4$ . This is precisely the scenario examined in this work.

By simple algebraic manipulation, the dispersion relation can be written in an equivalent series form [33]

$$\omega = \left(1 - \mathring{k}_{(I)}^{(4)}\right) |\mathbf{p}| \pm \mathring{k}_{(V)}^{(5)} \omega^2 - \mathring{k}_{(I)}^{(6)} \omega^3 \pm \mathring{k}_{(V)}^{(7)} \omega^4 - \mathring{k}_{(I)}^{(8)} \omega^5 \pm \dots \quad (17)$$

Recently, Ref. [44] restricted its analysis to the case  $d = 4$ , retaining only the coefficient  $\mathring{k}_{(I)}^{(4)}$  only. In that paper no birefringence nor anisotropies were reported. However, our current paper, let us consider the case where  $d > 4$ , i.e., which takes into account both operators  $\mathring{k}_{(I)}^{(4)}$  and  $\mathring{k}_{(V)}^{(5)}$ . This more involving configuration might produce more challenging aspects to deal with: anisotropies and birefringence, which will be investigated in the following sections.

The polarization states carried by gravitational waves provide direct access to both the properties of their sources and the symmetry principles underlying the gravitational interaction. When local Lorentz symmetry is not exact, its violation can leave characteristic signatures in the polarization sector, altering how different modes propagate and mix. As a result, measurements of gravitational wave polarization offer a sensitive observational window into both modified gravitational dynamics and nonstandard propagation effects [48–53].

We work within a weak-field regime in which gravitational waves propagate over a Minkowski background characterized by the metric  $\eta_{\mu\nu} = \text{diag}(-1, 1, 1, 1)$ . Focusing exclusively on the tensorial degrees of freedom, the spatial components of the metric fluctuation,  $h_{ij}(x)$  with indices  $i, j = 1, 2, 3$ , satisfy a wave equation whose form is altered by Lorentz-violating contributions arising in the linearized theory

$$(\partial_t^2 - \nabla^2) h_{ij}(x) + 2 \delta M_{ijmn}(\partial) h_{mn}(x) = 0. \quad (18)$$

All derivatives are defined with respect to the flat background geometry, so that  $\partial_t$  denotes differentiation with respect to the coordinate time  $t$  and the spatial Laplacian is given by  $\nabla^2 = \delta^{kl} \partial_k \partial_l$ .

Deviations from standard wave propagation are captured by the operator  $\delta M_{ijmn}(\partial)$ , which represents the Lorentz-violating corrections induced by higher-mass-dimension terms in the gravitational sector. Acting linearly on the tensor perturbations, this operator can include both CPT-even and CPT-odd contributions. Although these terms modify the dispersion and polarization behavior of gravitational waves, they do so without affecting the underlying Minkowski background structure.

The transverse traceless conditions continue to hold due to the residual gauge symmetry of the linearized theory

$$h_{ii} = 0, \quad \partial_i h_{ij} = 0. \quad (19)$$

Under these conditions, no independent scalar or vector modes propagate, and the physical content of the theory remains restricted to two tensorial degrees of freedom. The Lorentz-violating terms introduced in this analysis therefore do not enlarge the polarization basis. Instead, their influence is encoded in changes to the dispersion relations and in modifications to the way the existing tensor modes propagate through spacetime.

With this setup, the polarization structure can be examined by expressing the metric perturbation as a superposition of plane wave modes of the form

$$h_{\mu\nu}(x) = \varepsilon_{\mu\nu} e^{ip_\mu x^\mu}, \quad (20)$$

with

$$p^\mu = (\omega, 0, 0, p), \quad (21)$$

describing a wave traveling in the  $z$  direction. Imposing transversality with respect to the wave four-momentum, we obtain

$$p^\mu \varepsilon_{\mu\nu} = 0. \quad (22)$$

Notice that, when combined with the tracelessness condition  $\varepsilon^\mu{}_\mu = 0$ , these constraints restrict the polarization tensor to components that lie entirely within the spatial subspace and are orthogonal to the direction of propagation. As a result, only transverse spatial elements survive. Adopting the conventional linear polarization basis, the tensor structure can then be written as

$$\varepsilon_{\mu\nu} = \begin{pmatrix} 0 & 0 & 0 & 0 \\ 0 & \varepsilon_{11} & \varepsilon_{12} & 0 \\ 0 & \varepsilon_{12} & -\varepsilon_{11} & 0 \\ 0 & 0 & 0 & 0 \end{pmatrix}. \quad (23)$$

The quantities  $\varepsilon_{11}$  and  $\varepsilon_{12}$  parametrize the two independent degrees of freedom associated with the transverse traceless tensor sector. When CPT-odd Lorentz-violating operators with mass dimension  $d > 4$  are present, these amplitudes cease to remain fixed during propagation. Instead,

a relative phase develops between them, causing the polarization state to evolve dynamically. This effect manifests as a continuous rotation within the  $(+, \times)$  polarization basis as the gravitational wave travels through spacetime.

When Lorentz-violating operators of mass dimension  $d = 5$  are present, in particular those controlled by the CPT-odd coefficient  $\mathring{k}_{(V)}^{(5)}$ , the structure of the polarization tensor itself remains transverse and traceless, but the physical propagation eigenstates are no longer given by the linear  $(+, \times)$  modes. In other words, the modified dispersion relation,

$$\omega = \left(1 - \mathring{k}_{(I)}^{(4)}\right) |\mathbf{p}| \pm \mathring{k}_{(V)}^{(5)} \omega^2, \quad (24)$$

indicates that the two helicity states propagate differently. To leading order in Lorentz violation, this relation yields

$$\omega_\lambda \simeq \left(1 - \mathring{k}_{(I)}^{(4)}\right) |\mathbf{p}| + \lambda \mathring{k}_{(V)}^{(5)} |\mathbf{p}|^2, \quad \lambda = \pm 1, \quad (25)$$

where  $\lambda$  labels the right- and left-handed circular polarizations.

It is therefore convenient to introduce the circular polarization basis,

$$h_{R,L} = \frac{1}{\sqrt{2}}(h_+ \mp i h_\times), \quad (26)$$

which diagonalizes the propagation in the presence of the CPT-odd term. The two helicity modes acquire different phase velocities and accumulate a relative phase during propagation. After traveling a distance  $L$ , this phase difference is given by

$$\Delta\phi = (\omega_+ - \omega_-) L \simeq 2 \mathring{k}_{(V)}^{(5)} |\mathbf{p}|^2 L. \quad (27)$$

Transforming back to the linear polarization basis, the plus and cross amplitudes become mixed according to

$$\begin{pmatrix} h_+(L) \\ h_\times(L) \end{pmatrix} = \begin{pmatrix} \cos(\Delta\phi/2) & -\sin(\Delta\phi/2) \\ \sin(\Delta\phi/2) & \cos(\Delta\phi/2) \end{pmatrix} \begin{pmatrix} h_+(0) \\ h_\times(0) \end{pmatrix}. \quad (28)$$

This result shows that, although no additional tensor degrees of freedom are introduced, the presence of the  $d = 5$  CPT-odd operator leads to helicity-dependent propagation and induces a rotation of the polarization basis. As a consequence, an initially linearly polarized gravitational wave generally evolves into an elliptically polarized state. In other words, this phenomenon corresponds to gravitational wave birefringence and provides a fundamental observational signature of higher-dimension Lorentz-violating operators in the gravitational sector, as we shall be seeing in the forthcoming sections.

#### IV. GRAVITATIONAL WAVE EMISSION FROM MATTER SOURCES

To account for gravitational wave generation, the homogeneous equations governing metric perturbations are extended by coupling them to an external tensor source  $J_{ij}$ . Introducing this

current into the linearized framework defined by Eq. (18) converts the vacuum propagation equation into a sourced system, yielding the modified field equation

$$(\partial_t^2 - \nabla^2) h_{ij}(x) + 2\delta M_{ijmn}(\partial) h_{mn}(x) = J_{ij}(x). \quad (29)$$

The solution for the metric fluctuation follows by convolving the source with the retarded Green function associated with the modified wave operator, leading to

$$h_{ij}(x) = \sum_{\lambda=\pm} \int d^4y G_\lambda^{\text{ret}}(x-y) \Pi_{ijmn}^{(\lambda)} J_{mn}(y), \quad (30)$$

where  $G_\lambda^{\text{ret}}(x-y)$  denotes the retarded Green function associated with the helicity eigenmode  $\lambda = \pm$ , and  $\Pi_{ijmn}^{(\lambda)}$  is the transverse–traceless projector onto the corresponding circular polarization subspace. This decomposition makes explicit that, in the presence of CPT–odd Lorentz–violating operators, the two tensor helicities propagate independently with distinct dispersion relations, while the physical source entering the field equation is the transverse–traceless projection of the stress–energy tensor.

The construction of  $G^{\text{ret}}(x-y)$  is guided by the modified dispersion relation introduced in Eq. (17). Restricting to the isotropic Lorentz–violating coefficients  $\mathring{k}_{(I)}^{(4)}$  and  $\mathring{k}_{(V)}^{(5)}$ , the dispersion relation reads

$$\omega = p^0 = v|\vec{p}| \pm \mathring{k}_{(V)}^{(5)} \omega^2, \quad v \equiv 1 - \mathring{k}_{(I)}^{(4)}, \quad (31)$$

where the  $\pm$  sign labels the two circular polarization (helicity) states. In this isotropic truncation, Lorentz violation modifies the propagation speed and induces birefringence, but does not introduce directional anisotropies.

In Fourier space, the retarded Green function associated with each helicity mode is therefore given by

$$\tilde{G}_\pm^{\text{ret}}(p) = \frac{1}{(p^0)^2 - v^2|\vec{p}|^2 \mp 2\mathring{k}_{(V)}^{(5)}(p^0)^3 + i\epsilon p^0}, \quad (32)$$

where the  $i\epsilon p^0$  prescription enforces causal propagation.

Assuming  $|\mathring{k}_{(V)}^{(5)}| \ll 1$ , the Green function can be expanded perturbatively to first order as

$$\tilde{G}_\pm^{\text{ret}}(p) \simeq \frac{1}{(p^0)^2 - v^2|\vec{p}|^2 + i\epsilon p^0} \pm 2\mathring{k}_{(V)}^{(5)} \frac{(p^0)^3}{[(p^0)^2 - v^2|\vec{p}|^2 + i\epsilon p^0]^2}. \quad (33)$$

The inverse Fourier transform then yields

$$G_\pm^{\text{ret}}(t, \vec{x}) = \int \frac{dp^0}{2\pi} \int \frac{d^3p}{(2\pi)^3} e^{-ip^0t + i\vec{p}\cdot\vec{x}} \tilde{G}_\pm^{\text{ret}}(p). \quad (34)$$

Evaluating first the  $p^0$  integral by contour methods and closing the contour in the lower half–plane for  $t > 0$ , the leading contribution reproduces the standard retarded Green function with modified propagation speed  $v$ . The CPT–odd term proportional to  $\mathring{k}_{(V)}^{(5)}$  generates additional

contributions involving higher derivatives of the light–cone distribution. After performing the angular integrations and expressing the result in terms of distributions, the retarded Green function in coordinate space can be written as

$$G_{\pm}^{\text{ret}}(t, r) = \Theta(t) \frac{1}{4\pi r} \left[ \frac{1}{v^2} \delta\left(t - \frac{r}{v}\right) \pm \overset{\circ}{k}_{(V)}^{(5)} \left( \frac{2}{v^3} \delta'\left(t - \frac{r}{v}\right) + \frac{t}{v^4} \delta''\left(t - \frac{r}{v}\right) \right) \right], \quad r = |\vec{x}|. \quad (35)$$

This expression makes explicit the distinct roles of the Lorentz–violating coefficients. The coefficient  $\overset{\circ}{k}_{(I)}^{(4)}$  enters through the rescaling of the propagation speed  $v$ , leading to a shift in the retarded time, while the CPT–odd coefficient  $\overset{\circ}{k}_{(V)}^{(5)}$  induces helicity–dependent dispersive corrections encoded in higher derivatives of the light–cone delta distribution. By construction, the Green function satisfies the causal condition  $G_{\pm}^{\text{ret}}(t < 0, \vec{x}) = 0$  and reduces smoothly to the standard retarded Green function of general relativity in the limit  $\overset{\circ}{k}_{(I)}^{(4)}, \overset{\circ}{k}_{(V)}^{(5)} \rightarrow 0$ .

In the weak field regime of general relativity, the observable gravitational wave signal in the radiation zone is carried by the spatial components of the metric perturbation, whose leading contribution takes the form

$$h_{ij}(t, \mathbf{r}) = \frac{2G}{r} \frac{d^2 I_{ij}}{dt^2}(t_r), \quad (36)$$

with the retarded time defined as  $t_r = t - r/v$  and  $I_{ij}$  denoting the source’s mass quadrupole moment

$$I_{ij}(t) = \int y^i y^j T^{00}(t, \vec{y}) d^3 y. \quad (37)$$

Once Lorentz–violating contributions are introduced via the dispersion relation in Eq. (31), gravitational wave propagation is no longer governed by the standard retarded kernel but instead by the modified Green function given in Eq. (35). As a consequence, the metric perturbations sourced by matter differ from their general relativistic counterparts through two qualitatively distinct mechanisms.

One effect originates from the CPT–even, nondispersive coefficient  $\overset{\circ}{k}_{(I)}^{(4)}$ , which alters the effective speed at which gravitational waves propagate [44]. This modification can be parametrized as  $v \equiv 1 - \overset{\circ}{k}_{(I)}^{(4)}$ , leading to a corresponding shift in the retarded time,  $t_r = t - \frac{r}{v}$ . At the same time, the normalization of the retarded Green function introduces a global rescaling of the waveform amplitude by a factor  $1/v^2$  in the radiation zone. A second class of corrections arises from the CPT–odd, dispersive coefficient  $\overset{\circ}{k}_{(V)}^{(5)}$ . These contributions enter through higher–derivative structures proportional to  $\delta'$  and  $\delta''$  in Eq. (35), generating helicity–dependent modifications of the signal as well.

In this manner, the waveform can be written schematically as

$$h_{ij}(t, \mathbf{r}) = \frac{2G}{r} \left[ \frac{1}{v^2} \frac{d^2 I_{ij}}{dt^2}(t_r) \pm \overset{\circ}{k}_{(V)}^{(5)} \left( \frac{2}{v^3} \frac{d^3 I_{ij}}{dt^3}(t_r) + \frac{t_r}{v^4} \frac{d^4 I_{ij}}{dt^4}(t_r) \right) \right], \quad (38)$$

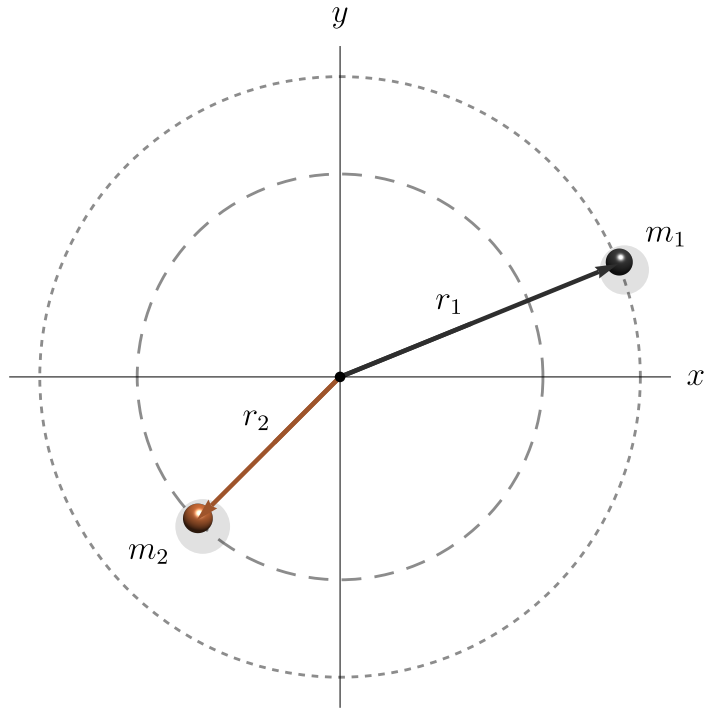


Figure 1: Illustration of a two-body black-hole system viewed in the barycentric frame. The compact constituents, labeled by masses  $m_1$  and  $m_2$ , undergo orbital motion restricted to the  $xy$  plane, with their trajectories specified by radii  $r_1$  and  $r_2$ .

where the waveform separates naturally into distinct pieces. The leading term coincides with the standard quadrupole expression, evaluated at a retarded time shifted by the effective propagation speed  $v$ , thereby encoding causal signal transmission at that speed [44]. The accompanying prefactor  $1/v^2$  originates from the normalization of the retarded Green function in the radiation zone. By contrast, the terms proportional to  $\mathring{k}_{(V)}^{(5)}$  introduce genuinely dispersive and birefringent effects, appearing through higher-order time derivatives of the mass quadrupole and modifying the temporal and polarization structure of the signal.

### A. Application with a binary black hole system

To illustrate these effects in a physical setting, we apply the formalism to a binary black hole system, schematically shown in Fig. 1. The configuration comprises two compact masses,  $m_1$  and  $m_2$ , undergoing orbital motion restricted to the  $xy$  plane. Adopting the center-of-mass frame, the motion of each body is characterized by its orbital radius, labeled  $r_1$  and  $r_2$ , which specify their trajectories about the common barycenter.

The gravitational radiation is generated by a simplified source model in which the system is represented by two pointlike bodies undergoing planar orbital motion. The influence of this matter configuration on the spacetime geometry is captured through the associated stress-energy

tensor, whose explicit form is given by

$$T_{00} = \delta(z) \left[ m_1 \delta(x - x_1) \delta(y - y_1) + m_2 \delta(x - x_2) \delta(y - y_2) \right]. \quad (39)$$

The binary dynamics are modeled by assuming that each constituent executes uniform circular motion around the system's barycenter. Within this approximation, the trajectories of the two bodies are specified by the relations

$$\begin{aligned} x_1(t) &= \frac{m_2 l_0}{M} \cos(\omega t), & y_1(t) &= \frac{m_2 l_0}{M} \sin(\omega t), \\ x_2(t) &= -\frac{m_1 l_0}{M} \cos(\omega t), & y_2(t) &= -\frac{m_1 l_0}{M} \sin(\omega t). \end{aligned} \quad (40)$$

Notice that, in this notation, the total mass of the system is  $M = m_1 + m_2$ , while the characteristic separation is given by  $l_0 = r_1 + r_2$ . The motion is assumed to be circular with angular velocity  $\omega$ , a choice that greatly simplifies the form of the mass quadrupole tensor. Under these assumptions, only three of its components remain nonvanishing,

$$\begin{aligned} I_{xx}(t) &= \frac{\mu}{2} l_0^2 [1 + \cos(2\omega t)], \\ I_{yy}(t) &= \frac{\mu}{2} l_0^2 [1 - \cos(2\omega t)], \\ I_{xy}(t) &= I_{yx}(t) = \frac{\mu}{2} l_0^2 \sin(2\omega t), \end{aligned} \quad (41)$$

where we have introduced the quantity the reduced mass  $\mu = m_1 m_2 / (m_1 + m_2)$ .

Inserting the explicit expressions for the quadrupole moments given in Eq. (41) into the waveform formula of Eq. (38), one finds that only a subset of the metric perturbation components survives in the radiation zone, namely

$$h_{xx}^{(\pm)}(t, r) = -\frac{4G \mu l_0^2 \omega^2}{r v^2} \cos(2\omega t_r) \pm \frac{16G \mu l_0^2}{r} \overset{\circ}{k}_{(V)}^{(5)} \left[ \frac{\omega^3}{v^3} \sin(2\omega t_r) + \frac{t_r \omega^4}{v^4} \cos(2\omega t_r) \right], \quad (42)$$

$$h_{yy}^{(\pm)}(t, r) = +\frac{4G \mu l_0^2 \omega^2}{r v^2} \cos(2\omega t_r) \pm \frac{16G \mu l_0^2}{r} \overset{\circ}{k}_{(V)}^{(5)} \left[ -\frac{\omega^3}{v^3} \sin(2\omega t_r) - \frac{t_r \omega^4}{v^4} \cos(2\omega t_r) \right], \quad (43)$$

$$h_{xy}^{(\pm)}(t, r) = h_{yx}^{(\pm)}(t, r) = -\frac{4G \mu l_0^2 \omega^2}{r v^2} \sin(2\omega t_r) \pm \frac{16G \mu l_0^2}{r} \overset{\circ}{k}_{(V)}^{(5)} \left[ -\frac{\omega^3}{v^3} \cos(2\omega t_r) + \frac{t_r \omega^4}{v^4} \sin(2\omega t_r) \right]. \quad (44)$$

These results make clear that the emitted signal retains the familiar tensorial structure associated with the quadrupole formula, even in the presence of Lorentz violation. The deviations instead arise through changes in how the waves propagate. One modification is controlled by the coefficient  $\overset{\circ}{k}_{(I)}^{(4)}$ , which alters the effective propagation speed  $v$ , thereby shifting the retarded

time at which the waveform is evaluated, as shown in the previous augmentations. The same coefficient also induces a uniform rescaling of the strain amplitude by a factor  $1/v^2$ , originating from the normalization of the retarded Green function. A second, qualitatively different effect is produced by the CPT-odd coefficient  $\mathring{k}_{(V)}^{(5)}$ . This term generates helicity-dependent dispersive corrections that enter through higher-order time derivatives of the mass quadrupole, reshaping the time dependence of the waveform while leaving the number of propagating degrees of freedom unchanged.

In Fig. 2, we display the waveform  $h_{xx}^+(t, r)$  as a function of the time  $t$  for a representative configuration of the system, namely  $\omega = 0.5$ ,  $r = 20$ ,  $\mu = 1$ , and  $l_0 = 1$ . As expected, the resulting signal encodes the combined effects of the Lorentz-violating coefficients  $\mathring{k}_{(I)}^{(4)}$  and  $\mathring{k}_{(V)}^{(5)}$ . The waveform exhibits a progressive distortion relative to the general-relativistic prediction as time evolves, reflecting the cumulative influence of the CPT-odd dispersive term on the phase and relative weights of the oscillatory components.

As recently reported in the literature [44], the coefficient  $\mathring{k}_{(I)}^{(4)}$  alone does not produce a modification of the gravitational wave amplitude; its effect is fully encoded through the retarded-time shift and the overall normalization governed by the effective velocity  $v$ . Accordingly, the additional time-dependent distortion observed when  $\mathring{k}_{(V)}^{(5)} \neq 0$  is associated with the CPT-odd contribution. To make this point more transparent, Fig. 3 shows separately the effects arising from  $\mathring{k}_{(I)}^{(4)}$  and  $\mathring{k}_{(V)}^{(5)}$ . In particular, the dependence on  $\mathring{k}_{(I)}^{(4)}$  is fully encoded through the effective velocity  $v$ , such that  $v = 1$  corresponds to the Lorentz-invariant limit  $\mathring{k}_{(I)}^{(4)} = 0$ .

Moreover, an important feature of Eqs. (42)–(44) deserves comment. For simplicity, we focus on Eq. (42); the same reasoning and conclusions apply straightforwardly to the remaining components. A characteristic aspect of the Lorentz-violating correction proportional to  $\mathring{k}_{(V)}^{(5)}$  is the appearance of a contribution linear in the retarded time  $t_r$ . As a result, the truncated first-order expression for the strain can develop a nonuniform envelope at sufficiently large  $|t_r|$ , with local extrema whose magnitude may increase as  $|t_r|$  grows. This behavior should not be interpreted as a physical amplification of the gravitational wave. Rather, it reflects the use of a monochromatic, infinite-duration source together with a perturbative expansion to first order in  $\mathring{k}_{(V)}^{(5)}$ , which is valid only while the Lorentz-violating correction remains small compared with the leading general-relativistic contribution.

To make this behavior explicit, it is convenient to rewrite the strain as

$$h_{xx}^{(\pm)}(t_r) = -C \cos(2\omega t_r) \pm D \left[ a \sin(2\omega t_r) + b t_r \cos(2\omega t_r) \right], \quad (45)$$

where

$$C = \frac{4G\mu l_0^2 \omega^2}{rv^2}, \quad D = \frac{16G\mu l_0^2}{r} \mathring{k}_{(V)}^{(5)}, \quad a = \frac{\omega^3}{v^3}, \quad b = \frac{\omega^4}{v^4}. \quad (46)$$

The extrema of  $h_{xx}^{(\pm)}$  are determined by  $dh_{xx}^{(\pm)}/dt_r = 0$ . For vanishing Lorentz violation, the extrema occur at  $t_{r,0} = n\pi/(2\omega)$  with  $n \in \mathbb{Z}$ . Treating the Lorentz-violating contribution perturbatively, the extrema are shifted according to

$$t_{r,n}^{(\text{ext})} \simeq \frac{n\pi}{2\omega} \mp \overset{\circ}{k}_{(V)}^{(5)} \frac{2v+1}{v^2}, \quad (47)$$

up to higher-order terms in  $\overset{\circ}{k}_{(V)}^{(5)}$ .

For the leading term  $-C \cos(2\omega t_r)$  with  $C > 0$ , the local minima correspond to  $\cos(2\omega t_r) = +1$ , namely even values  $n = 2m$ . The positions of the local minima are therefore given by

$$t_{r,m}^{(\text{min})} \simeq \frac{m\pi}{\omega} \mp \overset{\circ}{k}_{(V)}^{(5)} \frac{2v+1}{v^2}, \quad m \in \mathbb{Z}. \quad (48)$$

These expressions characterize the location of the extrema within the regime of validity of the perturbative expansion. In particular, the first-order treatment is reliable only while

$$\left| \overset{\circ}{k}_{(V)}^{(5)} \right| \frac{\omega^2}{v^2} |t_r| \ll 1, \quad (49)$$

up to factors of order unity. For realistic, finite-duration gravitational wave signals, this condition is naturally enforced by the limited observation time and by the time dependence of the orbital frequency, so that the Lorentz-violating effect manifests itself as a gradual distortion of the waveform rather than an unbounded growth.

Furthermore, the apparent reduction of the gravitational wave amplitude induced by the CPT-odd coefficient  $\overset{\circ}{k}_{(V)}^{(5)}$  should not be interpreted as a violation of energy conservation. The modified propagation governed by  $\overset{\circ}{k}_{(V)}^{(5)}$  is dispersive rather than dissipative, and the underlying effective theory remains invariant under time translations. As a consequence, the total energy carried by the gravitational wave is conserved. The observed modulation of the strain arises from helicity-dependent dispersion and phase distortion, which redistribute the waveform in time and among polarization components. In particular, when a single strain component or a monochromatic approximation is considered, this redistribution can manifest itself as an apparent attenuation of the signal. In other words, this effect reflects the fact that the plotted observable does not capture the full information content of the distorted waveform, instead of a genuine loss of gravitational wave energy.

In Fig. 3, we emphasize the impact of the operators  $\overset{\circ}{k}_{(I)}^{(4)}$  and  $\overset{\circ}{k}_{(V)}^{(5)}$  on the attenuation of gravitational waves, providing a complementary perspective to the behavior illustrated in Fig. 2.

In Fig. 4, we provide a parametric representation of the helicity (+) waveform in the  $(h_{xx}^+, h_{yx}^+)$  plane, which is equivalent to tracking the polarization state over one observation interval. The reference curve with  $\overset{\circ}{k}_{(V)}^{(5)} = 0$  (and  $v = 0.99$ ) forms a nearly circular trajectory, as expected for a standard monochromatic signal with a fixed phase relation between the two components.

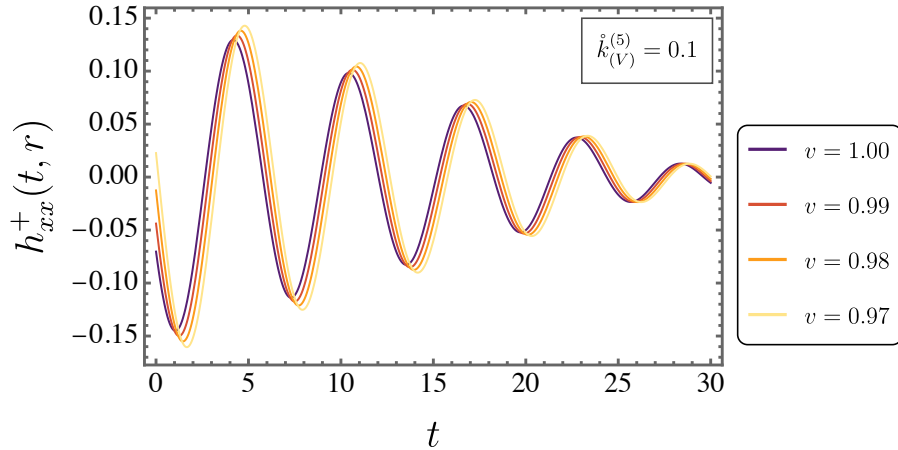


Figure 2: Waveform  $h_{xx}^+(t, r)$  as a function of time  $t$  for a representative configuration with  $\omega = 0.5$ ,  $r = 20$ ,  $\mu = 1$ , and  $l_0 = 1$ . The signal incorporates the combined effects of the Lorentz-violating coefficients  $\mathring{k}_{(I)}^{(4)}$  and  $\mathring{k}_{(V)}^{(5)}$ , and displays a clear attenuation characterized by a gradual decrease of the amplitude as time evolves.

When the CPT-odd coefficient  $\mathring{k}_{(V)}^{(5)}$  is switched on (here  $\mathring{k}_{(V)}^{(5)} = 0.1$  with  $v = 1$ ), the orbit is visibly distorted and becomes non-closed, reflecting the dispersive phase distortion and the drift produced by the first-order  $d = 5$  correction. In particular, the drift of the curve and the progressive deformation of the loop provide a complementary visualization of the propagation-induced waveform distortion already displayed in Fig. 2.

Figure 5 displays the transverse deformation of a ring of freely falling test particles produced by a gravitational wave propagating along the orthogonal direction. Each panel corresponds to a fixed value of the retarded phase  $\phi = 2\omega t_r$ , where  $t_r = t - r/v$ , and the sequence of snapshots spans one complete oscillation period. In all panels, the dashed circle represents the undeformed configuration of the ring in the absence of the gravitational wave. The solid curves depict the instantaneous displacement of the particles obtained from the linearized transverse-traceless mapping  $x^i \rightarrow x^i + \frac{1}{2}h^i_j x^j$ , with the nonvanishing strain components given by  $h_{xx}$  and  $h_{yy}$ . The small markers highlight selected test particles initially located along the principal axes of the ring, allowing the stretching and squeezing directions to be clearly identified at each phase; white circular markers correspond to the Lorentz-violating configuration, while black dots denote the reference case. The parameters used in the plots are  $\mu = 1$ ,  $l_0 = 1$ ,  $\omega = 0.5$ , and  $r = 20$ . The black solid curve represents the reference configuration with  $\mathring{k}_{(V)}^{(5)} = 0$  and propagation speed  $v = 0.99$ , whereas the wine-colored curve corresponds to the Lorentz-violating case with  $\mathring{k}_{(V)}^{(5)} = 0.1$  and  $v = 1$ . As the phase evolves, the ring is distorted into elliptic shapes whose orientation and eccentricity change over the cycle, illustrating the polarization-state evolution induced by helicity-dependent  $d = 5$  CPT-odd propagation.

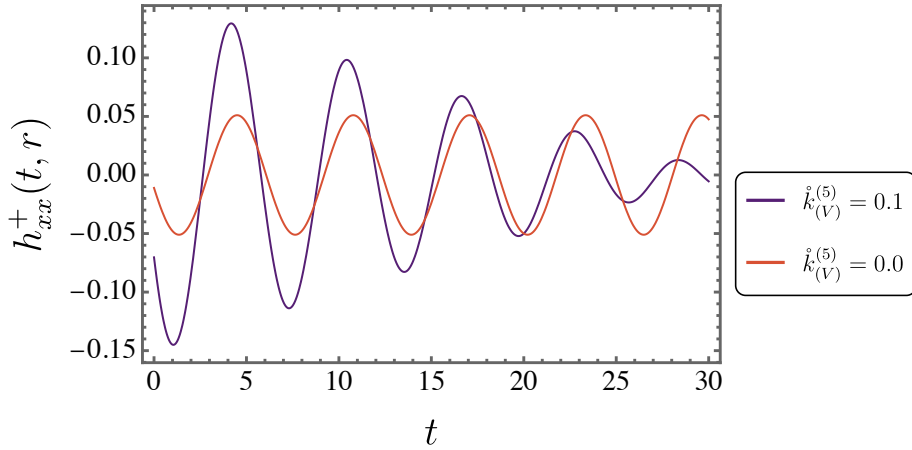


Figure 3: Impact of the Lorentz-violating operators  $\mathring{k}_{(I)}^{(4)}$  and  $\mathring{k}_{(V)}^{(5)}$  on the attenuation of gravitational waves, as illustrated by the corresponding waveform behavior.

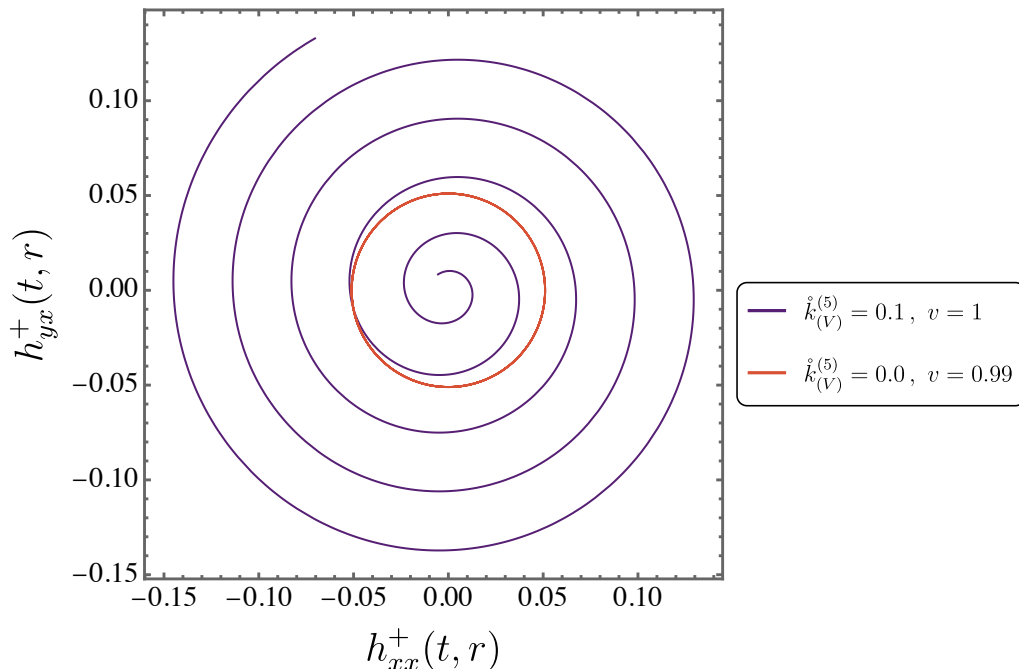


Figure 4: Parametric plot of the helicity (+) waveform in the  $(h_{xx}^+, h_{yx}^+)$  plane, tracing the polarization state over one observation interval. The reference case with  $\mathring{k}_{(V)}^{(5)} = 0$  and  $v = 0.99$  yields an almost circular trajectory, characteristic of a monochromatic signal with a fixed phase relation between components. When the CPT-odd coefficient  $\mathring{k}_{(V)}^{(5)}$  is included ( $\mathring{k}_{(V)}^{(5)} = 0.1$ ,  $v = 1$ ), the trajectory becomes distorted and non-closed, with a noticeable drift and loop deformation that signal time-dependent phase and amplitude modifications associated with altered wave propagation.

## V. BOUNDS FROM LVK (VIRGO/KAGRA-INCLUDING CATALOGS) DATA

This section updates the phenomenological bounds on the isotropic propagation coefficients by using *published constraints inferred from LIGO-Virgo-KAGRA (LVK) analyses*. We emphasize

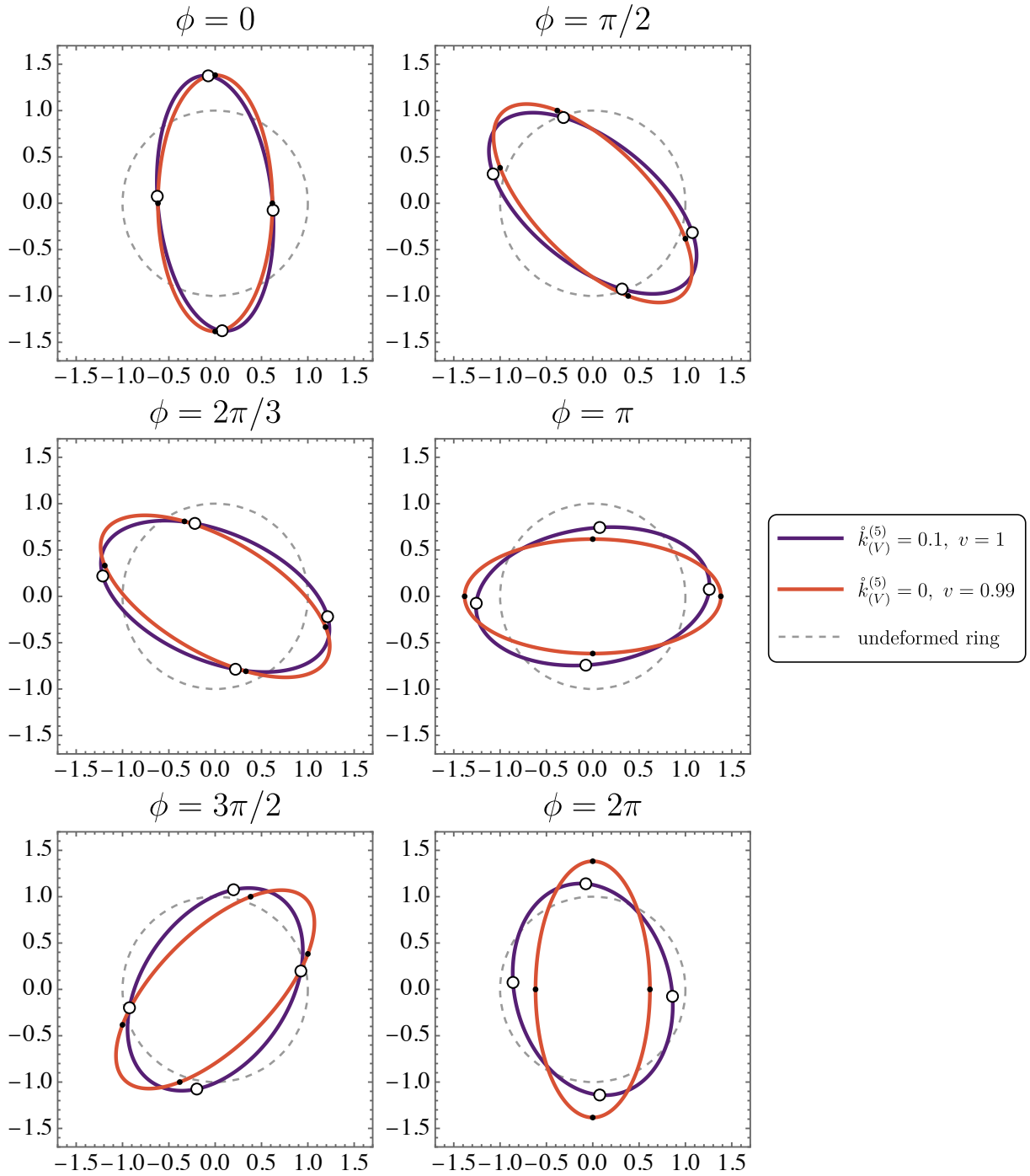


Figure 5: Transverse deformation of a ring of freely falling test particles induced by a gravitational wave. Snapshots are shown at fixed retarded phase  $\phi = 2\omega t_r$ , with  $t_r = t - r/v$ , over one oscillation period. The dashed circle denotes the undeformed ring, while solid curves show the instantaneous displacement from the transverse–traceless mapping with nonzero components  $h_{xx}$  and  $h_{yx}$ . Markers indicate selected particles along the principal axes (white: Lorentz–violating case; black: reference). Parameters are  $\mu = 1$ ,  $l_0 = 1$ ,  $\omega = 0.5$ , and  $r = 20$ . The black curve corresponds to  $\dot{k}_{(V)}^{(5)} = 0$ ,  $v = 0.99$ , and the wine–colored curve to  $\dot{k}_{(V)}^{(5)} = 0.1$ ,  $v = 1$ , illustrating birefringent distortions over the cycle.

that we do not reanalyze the strain data here; instead, we translate the LVK posterior constraints reported in the official catalogs and “Tests of General Relativity” analyses into bounds on  $\mathring{k}_{(I)}^{(4)}$  and  $\mathring{k}_{(V)}^{(5)}$  [54–56].

### A. Bound on the nondispersive coefficient $\mathring{k}_{(I)}^{(4)}$

In our isotropic parametrization, the nondispersive coefficient is encoded through

$$v \equiv 1 - \mathring{k}_{(I)}^{(4)}, \quad \Rightarrow \quad \left| \mathring{k}_{(I)}^{(4)} \right| = \frac{|v - c|}{c}. \quad (50)$$

A robust LVK bound comes from the multimessenger association GW170817/GRB 170817A, observed by the Advanced LIGO and Advanced Virgo detectors, which constrains the fractional difference between the GW speed and the speed of light to be [55]

$$-3 \times 10^{-15} \lesssim \frac{v - c}{c} \lesssim 7 \times 10^{-16}. \quad (51)$$

Therefore, within the present isotropic model,

$$\boxed{\left| \mathring{k}_{(I)}^{(4)} \right| \lesssim 3 \times 10^{-15}.} \quad (52)$$

For comparison, independent bounds obtained from detector-network timing using GW observations alone (without electromagnetic counterparts) yield significantly weaker constraints, typically  $v \simeq (0.97\text{--}1.01)c$  when combining O1–O2 events [54], and therefore do not compete with the multimessenger limit.

### B. Bounds on the CPT-odd $d = 5$ coefficient $\mathring{k}_{(V)}^{(5)}$

#### 1. Translation from LVK parameterized dispersion tests

To connect our  $d = 5$  CPT-odd term with LVK propagation tests, we employ the standard parameterized modified dispersion relation adopted in the LVK “Tests of GR” framework [56],

$$E^2 = p^2 c^2 + A_\alpha p^\alpha c^\alpha, \quad (53)$$

where constraints on  $A_\alpha$  are obtained by combining multiple events across the LVK catalogs.

For  $\alpha = 3$ , Eq. (53) yields (in units with  $c = \hbar = 1$ )

$$\omega^2 = p^2 + A_3 p^3 \quad \Rightarrow \quad \omega \simeq p + \frac{1}{2} A_3 p^2, \quad (54)$$

to leading order in  $A_3$ .

On the other hand, the helicity-resolved dispersion relation derived in this work takes the form

$$\omega_\lambda \simeq (1 - \mathring{k}_{(I)}^{(4)})p + \lambda \mathring{k}_{(V)}^{(5)} p^2, \quad \lambda = \pm 1. \quad (55)$$

Neglecting the tiny overall rescaling induced by  $\mathring{k}_{(I)}^{(4)}$  in this matching step, the LVK *nonbirefringent* coefficient  $A_3$  constrains the magnitude of any  $p^2$  correction to the phase velocity. A conservative translation is therefore obtained by identifying the size of the  $p^2$  term,

$$\boxed{\left| \mathring{k}_{(V)}^{(5)} \right| \lesssim \frac{|A_3|}{2}}. \quad (56)$$

This estimate is conservative, since the LVK  $A_3$  analysis is not optimized for helicity-dependent birefringence; a dedicated birefringent waveform template would be expected to constrain  $\mathring{k}_{(V)}^{(5)}$  more directly [33, 37].

*a. Numerical value from GWTC-3 propagation bounds.* The LVK propagation tests reported in GWTC-3 constrain the dimensionless quantity  $\bar{A}_\alpha \equiv A_\alpha/\text{eV}^{2-\alpha}$  [56]. For  $\alpha = 3$ , the combined 90% credible bound reads

$$|\bar{A}_3| \lesssim (0.45\text{--}1.16) \times 10^{-2}. \quad (57)$$

Converting back,

$$|A_3| \lesssim (0.45\text{--}1.16) \times 10^{-2} \text{ eV}^{-1}. \quad (58)$$

Using  $1 \text{ eV}^{-1} \simeq 6.582 \times 10^{-16} \text{ s}$ , Eq. (56) yields

$$\boxed{\left| \mathring{k}_{(V)}^{(5)} \right| \lesssim (1.5\text{--}3.8) \times 10^{-18} \text{ s}, \quad (90\% \text{ C.I., LVK GWTC-3 translation})}. \quad (59)$$

## 2. Birefringent phase accumulation

An independent and physically transparent constraint on  $\mathring{k}_{(V)}^{(5)}$  follows from the absence of large polarization rotation in observed GW signals. The helicity-dependent dispersion relation implies an accumulated relative phase

$$\Delta\phi = (\omega_+ - \omega_-) L \simeq 2 \mathring{k}_{(V)}^{(5)} \omega^2 L, \quad (60)$$

which induces mixing between the  $(+, \times)$  polarization states during propagation [33].

Requiring that the accumulated birefringent phase remains smaller than an  $\mathcal{O}(1)$  tolerance,

$$|\Delta\phi| \lesssim 1, \quad (61)$$

yields the conservative bound

$$\boxed{\left| \mathring{k}_{(V)}^{(5)} \right| \lesssim \frac{1}{2\omega^2 L}}. \quad (62)$$

For representative LVK sources with  $f \sim 100$  Hz and distances  $L \sim 40\text{--}500$  Mpc, this estimate leads to bounds that are consistent with, though typically weaker than, the catalog-level constraint in Eq. (59). Importantly, Eq. (62) directly probes the distinctive birefringent signature of the CPT-odd  $d = 5$  operator and is closely tied to the regime of validity of the perturbative waveform expansion derived in this work.

Collecting the results, a consistent set of bounds for the isotropic coefficients is

$$\boxed{\left| \overset{\circ}{k}_{(I)}^{(4)} \right| \lesssim 3 \times 10^{-15}} \quad (\text{GW170817/GRB 170817A; LV}), \quad (63)$$

$$\boxed{\left| \overset{\circ}{k}_{(V)}^{(5)} \right| \lesssim (1.5\text{--}3.8) \times 10^{-18} \text{ s}} \quad (\text{LVK GWTC-3 propagation tests}), \quad (64)$$

$$\boxed{\left| \overset{\circ}{k}_{(V)}^{(5)} \right| \lesssim \frac{1}{2\omega^2 L}} \quad (\text{birefringent phase consistency bound}). \quad (65)$$

In principle, these bounds can be inserted directly into our waveform expressions and into the polarization-mixing phase  $\Delta\phi$  to verify that the perturbative regime and the absence of large birefringent rotation remain compatible with current LVK observations.

### 3. Strain-based effects

The bounds above rely on catalog-level propagation analyses and on phase-accumulation arguments. One can also obtain complementary *strain-based* consistency bounds by using the fact that LVK observations show that the measured strain is well described by GR templates, with no statistically significant evidence for additional growth or polarization anomalies. In what follows we do not reanalyze detector data; instead, we impose conservative requirements directly on the analytic strain components (42)–(44).

*a. Term control in  $h_{ij}^{(\pm)}$ .* From Eqs. (42)–(44), the  $d = 5$  contribution contains a term proportional to  $t_r\omega^4$ , which is the dominant correction at sufficiently late retarded times  $t_r$ . A conservative requirement is that the Lorentz-violating correction never exceeds a small fraction  $\epsilon \ll 1$  of the leading GR term over the portion of the signal used in matched filtering,

$$\max_{t_r \in [0, T]} \left| \frac{h_{ij}^{(5)}(t_r)}{h_{ij}^{(0)}(t_r)} \right| \lesssim \epsilon, \quad (66)$$

where  $T$  is an effective signal duration (e.g., the analysis window) and  $h_{ij}^{(0)}$  denotes the  $k_{(V)}^{(5)} = 0$  piece.

Using (42) as representative, and keeping the dominant late-time piece,

$$\left| \frac{h_{xx}^{(5)}}{h_{xx}^{(0)}} \right| \sim 4 \left| \overset{\circ}{k}_{(V)}^{(5)} \right| \frac{\omega}{v} \left[ 1 + \frac{t_r\omega}{v} \right], \quad (67)$$

so that the contribution implies the bound

$$\boxed{\left| \dot{k}_{(V)}^{(5)} \right| \lesssim \frac{\epsilon}{4} \frac{v^2}{T \omega^2}} \quad (\text{term strain consistency}). \quad (68)$$

This constraint is independent of the source distance  $r$  because both the GR and  $d = 5$  pieces scale as  $1/r$  in Eqs. (42)–(44). It is therefore best interpreted as a *template-validity* bound on  $\dot{k}_{(V)}^{(5)}$  for a signal of duration  $T$  in the LVK band.

*b. Envelope / amplitude-modulation bound.* A second way to phrase the same idea is to require that the LV correction does not introduce an observable envelope modulation of the strain beyond a tolerance set by detector sensitivity. Let  $\rho$  denote the network signal-to-noise ratio (SNR) for a given event. A conservative criterion for the absence of additional modulation in matched-filtering analyses is that the fractional amplitude deformation remains below the statistical scale  $\sim 1/\rho$ ,

$$\max_{t_r \in [0, T]} \left| \frac{\delta h(t_r)}{h(t_r)} \right| \lesssim \frac{1}{\rho}. \quad (69)$$

Applying (69) to the dominant part of (42) yields

$$\boxed{\left| \dot{k}_{(V)}^{(5)} \right| \lesssim \frac{1}{4\rho} \frac{v^2}{T \omega^2}} \quad (\text{SNR-based strain bound}). \quad (70)$$

This estimate becomes more restrictive for louder signals (larger  $\rho$ ) and for longer signals (larger  $T$ ), as expected.

*c. Strain-based bound on  $\dot{k}_{(I)}^{(4)}$  from timing across the detector network.* Even without electromagnetic counterparts, the LVK strain data constrain the propagation speed through the relative arrival times across geographically separated detectors. If  $\Delta t_{\text{net}}$  denotes the characteristic uncertainty with which an event’s arrival time is reconstructed by a network (set by timing triangulation and the waveform bandwidth), a conservative bound is

$$\left| \frac{v - c}{c} \right| \lesssim \frac{\Delta t_{\text{net}}}{L/c}, \quad (71)$$

where  $L$  is the source distance. In our parametrization this translates to

$$\boxed{\left| \dot{k}_{(I)}^{(4)} \right| \lesssim \frac{c \Delta t_{\text{net}}}{L}} \quad (\text{strain-only network timing bound}). \quad (72)$$

This type of constraint is the one underlying the GW-only bounds reported in early LVK tests of GR [54], and is typically much weaker than the multimessenger limit (52).

*d. Relation to the birefringent phase bound.* The phase-accumulation bound (62) probes propagation over the full distance  $L$  through  $\Delta\phi \propto \omega^2 L$ . In contrast, the strain-based bounds (68) and (70) constrain the absence of amplitude deformation within the *observed time window*  $T$ . These constraints are therefore complementary: the former is controlled by  $L$ , while the latter is controlled by  $T$  (and potentially by  $\rho$  through (70)).

*e. Numerical illustration using benchmark LVK events.* Although we do not reanalyze the detector strain, it is useful to attach indicative numbers to the strain-based bounds by adopting representative event characteristics reported by the LVK Collaboration. For the first BBH detection GW150914, the observed peak strain is of order  $h_{\text{peak}} \sim 10^{-21}$  and the combined matched-filter SNR is  $\rho \simeq 24$  [54]. For the BNS event GW170817, the strain amplitude is of order  $10^{-22}$  and the combined network SNR is  $\rho \simeq 32.4$  [55].

To evaluate the strain-consistency bound (70), we adopt a representative gravitational wave frequency  $f \sim 100$  Hz (so that  $\omega = \pi f$  in our notation, since the oscillatory terms in (42)–(44) involve  $\cos(2\omega t_r)$  and  $\sin(2\omega t_r)$ ), and choose an effective in-band duration  $T$ . For BBH mergers, a conservative choice is  $T \sim 0.1$ – $0.3$  s, while for BNS inspirals one may take  $T \sim 10^2$  s as a representative time spent in band prior to merger [55]. Setting  $v \simeq 1$ , Eq. (70) gives

$$\left| \mathring{k}_{(V)}^{(5)} \right| \lesssim \frac{1}{4\rho T \omega^2} \sim 5 \times 10^{-7} \text{ s} \quad (\text{GW150914-like: } \rho \simeq 24, T \simeq 0.2 \text{ s}, f \simeq 100 \text{ Hz}), \quad (73)$$

$$\left| \mathring{k}_{(V)}^{(5)} \right| \lesssim \frac{1}{4\rho T \omega^2} \sim 8 \times 10^{-10} \text{ s} \quad (\text{GW170817-like: } \rho \simeq 32.4, T \simeq 100 \text{ s}, f \simeq 100 \text{ Hz}). \quad (74)$$

These strain-based consistency estimates are typically much weaker than the catalog-level propagation constraint (59), which is expected because (70) is designed primarily to control growth within the analysis window and to ensure the perturbative validity of Eqs. (42)–(44), rather than to compete with dedicated LVK propagation fits.

## VI. CONCLUSION

In this work, we analyzed how Lorentz- and diffeomorphism-violating operators in the linearized gravitational sector of the Standard Model Extension modified the propagation of gravitational waves. Restricting attention to the transverse-traceless tensor sector and to isotropic coefficients, we focused on the combined effects of the nondispersive CPT-even dimension-four coefficient  $\mathring{k}_{(I)}^{(4)}$  and the CPT-odd dimension-five coefficient  $\mathring{k}_{(V)}^{(5)}$ .

Starting from the quadratic action for metric perturbations, we derived the modified dispersion relation and showed that Lorentz violation altered gravitational wave propagation through two distinct mechanisms. The coefficient  $\mathring{k}_{(I)}^{(4)}$  rescaled the propagation speed, leading to a shift in the retarded time and an overall amplitude rescaling of the waveform. In contrast, the CPT-odd coefficient  $\mathring{k}_{(V)}^{(5)}$  introduced helicity-dependent dispersive effects, giving rise to birefringence and polarization mixing without activating additional propagating degrees of freedom.

We constructed the retarded Green function associated with the modified wave operator and obtained explicit expressions for the gravitational waveform generated by matter sources. When applied to a binary black hole system, the resulting radiation preserved the standard quadrupole

tensorial structure but acquired characteristic propagation–induced distortions. These included higher time–derivative corrections to the quadrupole formula, helicity–dependent phase shifts, and an attenuation of the strain amplitude. We emphasized that this attenuation did not signal a violation of energy conservation, but rather reflected energy exchange between the propagating gravitational wave and the fixed Lorentz–violating background encoded in the effective field–theory description.

Using published LIGO–Virgo–KAGRA propagation tests, polarization consistency arguments, and strain–based considerations, we translated current observational results into bounds on the isotropic coefficients. The multimessenger event GW170817 constrained the nondispersive coefficient to  $|\mathring{k}_{(I)}^{(4)}| \lesssim 3 \times 10^{-15}$ , while LVK catalog–level propagation tests and birefringent phase accumulation arguments yielded bounds on the CPT–odd coefficient at the level  $|\mathring{k}_{(V)}^{(5)}| \lesssim 10^{-18}$  s. Complementary strain–based estimates provided additional consistency conditions ensuring the perturbative validity of the derived waveforms.

As a further perspective, it would be worthwhile to examine the role of the remaining Lorentz–violating coefficients, for instance  $\mathring{k}_{(I)}^{(6)}$ ,  $\mathring{k}_{(V)}^{(7)}$ , and  $\mathring{k}_{(I)}^{(8)}$ , either separately or in suitable combinations. Such an analysis may uncover new or additional effects associated with birefringence and with the propagation properties of gravitational waves. Since these higher–dimension coefficients enter at progressively higher powers of the frequency  $\omega$ , identifying which ones are responsible for the expected dispersive behavior is particularly relevant. In addition, exploring the modified dispersion relations derived here within the framework of ensemble theory appears to be a natural direction for future work, as discussed in Refs. [57–61].

## VII. ACKNOWLEDGMENTS

A. A. Araújo Filho is supported by Conselho Nacional de Desenvolvimento Científico e Tecnológico (CNPq) and Fundação de Apoio à Pesquisa do Estado da Paraíba (FAPESQ), project numbers 150223/2025-0 and 1951/2025. N. Heidari is supported by Conselho Nacional de Desenvolvimento Científico e Tecnológico (CNPq) with the project number being 152891/2025-0. I. P. L. was partially supported by the National Council for Scientific and Technological Development - CNPq, grant 312547/2023-4 and to acknowledge networking support by the COST Action BridgeQG (CA23130), the COST Action RQI (CA23115) and the COST Action FuSe (CA24101) supported by COST (European Cooperation in Science and Technology).

## VIII. DATA AVAILABILITY STATEMENT

Data Availability Statement: No Data associated in the manuscript

---

- [1] R. N. Manchester, “Pulsars and Gravity,” *Int. J. Mod. Phys. D*, vol. 24, no. 06, p. 1530018, 2015.
- [2] C. M. Will, “Bounding the mass of the graviton using gravitational wave observations of inspiralling compact binaries,” *Phys. Rev. D*, vol. 57, pp. 2061–2068, 1998.
- [3] C. D. Hoyle, U. Schmidt, B. R. Heckel, E. G. Adelberger, J. H. Gundlach, D. J. Kapner, and H. E. Swanson, “Submillimeter tests of the gravitational inverse square law: a search for ‘large’ extra dimensions,” *Phys. Rev. Lett.*, vol. 86, pp. 1418–1421, 2001.
- [4] B. Jain and J. Khoury, “Cosmological Tests of Gravity,” *Annals Phys.*, vol. 325, pp. 1479–1516, 2010.
- [5] T. Clifton, P. G. Ferreira, A. Padilla, and C. Skordis, “Modified Gravity and Cosmology,” *Phys. Rept.*, vol. 513, pp. 1–189, 2012.
- [6] K. Koyama, “Cosmological Tests of Modified Gravity,” *Rept. Prog. Phys.*, vol. 79, no. 4, p. 046902, 2016.
- [7] I. H. Stairs, “Testing general relativity with pulsar timing,” *Living Rev. Rel.*, vol. 6, p. 5, 2003.
- [8] N. Wex, “Testing Relativistic Gravity with Radio Pulsars,” 2 2014.
- [9] M. Kramer, “Pulsars as probes of gravity and fundamental physics,” *Int. J. Mod. Phys. D*, vol. 25, no. 14, p. 1630029, 2016.
- [10] E. Berti *et al.*, “Testing General Relativity with Present and Future Astrophysical Observations,” *Class. Quant. Grav.*, vol. 32, p. 243001, 2015.
- [11] V. A. Kostelecky and S. Samuel, “Spontaneous Breaking of Lorentz Symmetry in String Theory,” *Phys. Rev. D*, vol. 39, p. 683, 1989.
- [12] V. A. Kostelecky and R. Potting, “CPT and strings,” *Nucl. Phys. B*, vol. 359, pp. 545–570, 1991.
- [13] R. Gambini and J. Pullin, “Nonstandard optics from quantum space-time,” *Phys. Rev. D*, vol. 59, p. 124021, 1999.
- [14] C. P. Burgess, J. M. Cline, E. Filotas, J. Matias, and G. D. Moore, “Loop generated bounds on changes to the graviton dispersion relation,” *JHEP*, vol. 03, p. 043, 2002.
- [15] D. Colladay and V. A. Kostelecky, “CPT violation and the standard model,” *Phys. Rev. D*, vol. 55, pp. 6760–6774, 1997.
- [16] V. A. Kostelecky, “Gravity, Lorentz violation, and the standard model,” *Phys. Rev. D*, vol. 69, p. 105009, 2004.

- [17] A. Bourgoin, C. Le Poncin-Lafitte, A. Hees, S. Bouquillon, G. Francou, and M.-C. Angonin, “Lorentz Symmetry Violations from Matter-Gravity Couplings with Lunar Laser Ranging,” *Phys. Rev. Lett.*, vol. 119, no. 20, p. 201102, 2017.
- [18] J. B. R. Battat, J. F. Chandler, and C. W. Stubbs, “Testing for Lorentz Violation: Constraints on Standard-Model Extension Parameters via Lunar Laser Ranging,” *Phys. Rev. Lett.*, vol. 99, p. 241103, 2007.
- [19] H. Muller, S.-w. Chiow, S. Herrmann, S. Chu, and K.-Y. Chung, “Atom Interferometry tests of the isotropy of post-Newtonian gravity,” *Phys. Rev. Lett.*, vol. 100, p. 031101, 2008.
- [20] V. A. Kostelecký and J. D. Tasson, “Constraints on Lorentz violation from gravitational Čerenkov radiation,” *Phys. Lett. B*, vol. 749, pp. 551–559, 2015.
- [21] L. Shao, “Tests of local Lorentz invariance violation of gravity in the standard model extension with pulsars,” *Phys. Rev. Lett.*, vol. 112, p. 111103, 2014.
- [22] L. Shao, “Lorentz-Violating Matter-Gravity Couplings in Small-Eccentricity Binary Pulsars,” *Symmetry*, vol. 11, no. 9, p. 1098, 2019.
- [23] L. Shao, “New pulsar limit on local Lorentz invariance violation of gravity in the standard-model extension,” *Phys. Rev. D*, vol. 90, no. 12, p. 122009, 2014.
- [24] L. Shao and Q. G. Bailey, “Testing the Gravitational Weak Equivalence Principle in the Standard-Model Extension with Binary Pulsars,” *Phys. Rev. D*, vol. 99, no. 8, p. 084017, 2019.
- [25] R. J. Jennings, J. D. Tasson, and S. Yang, “Matter-Sector Lorentz Violation in Binary Pulsars,” *Phys. Rev. D*, vol. 92, no. 12, p. 125028, 2015.
- [26] L. Shao and Q. G. Bailey, “Testing velocity-dependent CPT-violating gravitational forces with radio pulsars,” *Phys. Rev. D*, vol. 98, no. 8, p. 084049, 2018.
- [27] A. Hees, Q. G. Bailey, C. Le Poncin-Lafitte, A. Bourgoin, A. Rivoldini, B. Lamine, F. Meynadier, C. Guerlin, and P. Wolf, “Testing Lorentz symmetry with planetary orbital dynamics,” *Phys. Rev. D*, vol. 92, no. 6, p. 064049, 2015.
- [28] N. A. Flowers, C. Goodge, and J. D. Tasson, “Superconducting-Gravimeter Tests of Local Lorentz Invariance,” *Phys. Rev. Lett.*, vol. 119, no. 20, p. 201101, 2017.
- [29] A. V. Kostelecky and J. D. Tasson, “Matter-gravity couplings and Lorentz violation,” *Phys. Rev. D*, vol. 83, p. 016013, 2011.
- [30] Q. G. Bailey and V. A. Kostelecky, “Signals for Lorentz violation in post-Newtonian gravity,” *Phys. Rev. D*, vol. 74, p. 045001, 2006.
- [31] V. A. Kostelecký and M. Mewes, “Lorentz and Diffeomorphism Violations in Linearized Gravity,” *Phys. Lett. B*, vol. 779, pp. 136–142, 2018.
- [32] A. F. Ferrari, M. Gomes, J. R. Nascimento, E. Passos, A. Y. Petrov, and A. J. da Silva, “Lorentz

- violation in the linearized gravity,” *Phys. Lett. B*, vol. 652, pp. 174–180, 2007.
- [33] V. A. Kostelecký and M. Mewes, “Testing local Lorentz invariance with gravitational waves,” *Phys. Lett. B*, vol. 757, pp. 510–514, 2016.
- [34] S. Hou, X.-L. Fan, T. Zhu, and Z.-H. Zhu, “Nontensorial gravitational wave polarizations from the tensorial degrees of freedom: Linearized Lorentz-violating theory of gravity,” *Phys. Rev. D*, vol. 109, no. 8, p. 084011, 2024.
- [35] Y. Dong, Z. Wang, and L. Shao, “New limits on the local Lorentz invariance violation of gravity in the standard model extension with pulsars,” *Phys. Rev. D*, vol. 109, no. 8, p. 084024, 2024.
- [36] T. Zhu, W. Zhao, J.-M. Yan, Y.-Z. Wang, C. Gong, and A. Wang, “Constraints on parity and Lorentz violations in gravity from GWTC-3 through a parametrization of modified gravitational wave propagations,” *Phys. Rev. D*, vol. 110, no. 6, p. 064044, 2024.
- [37] M. Mewes, “Signals for Lorentz violation in gravitational waves,” *Phys. Rev. D*, vol. 99, no. 10, p. 104062, 2019.
- [38] L. Haegel, K. O’Neal-Ault, Q. G. Bailey, J. D. Tasson, M. Bloom, and L. Shao, “Search for anisotropic, birefringent spacetime-symmetry breaking in gravitational wave propagation from GWTC-3,” *Phys. Rev. D*, vol. 107, no. 6, p. 064031, 2023.
- [39] K. O’Neal-Ault, Q. G. Bailey, T. Dumerchat, L. Haegel, and J. Tasson, “Analysis of Birefringence and Dispersion Effects from Spacetime-Symmetry Breaking in Gravitational Waves,” *Universe*, vol. 7, no. 10, p. 380, 2021.
- [40] Q. G. Bailey, A. S. Gard, N. A. Nilsson, R. Xu, and L. Shao, “Classical radiation fields for scalar, electromagnetic, and gravitational waves with spacetime-symmetry breaking,” *Annals Phys.*, vol. 461, p. 169582, 2024.
- [41] N. A. Nilsson and C. L.-P. Lafitte, “Spacetime symmetry breaking effects in gravitational-wave generation at the first post-Newtonian order,” *Phys. Rev. D*, vol. 109, no. 2, p. 024035, 2024.
- [42] S. Aoulad Lafkih, M.-C. Angonin, C. Le Poncin-Lafitte, and N. A. Nilsson, “Gravitational-wave generation in the presence of Lorentz invariance violation,” 6 2025.
- [43] T.-C. Li, T. Zhu, W. Zhao, and A. Wang, “Power spectra and circular polarization of primordial gravitational waves with parity and Lorentz violations,” *JCAP*, vol. 07, p. 005, 2024.
- [44] A. A. Araújo Filho, N. Heidari, and I. P. Lobo, “Gravitational waves in a minimal gravitational SME,” 2 2026.
- [45] K. M. Amarilo, M. B. Ferreira Filho, A. A. Araújo Filho, and J. A. A. S. Reis, “Gravitational waves effects in a lorentz–violating scenario,” *Physics Letters B*, vol. 855, p. 138785, 2024.
- [46] Q. Wang, J.-M. Yan, T. Zhu, and W. Zhao, “Modified gravitational wave propagations in linearized gravity with Lorentz and diffeomorphism violations and their gravitational wave constraints,” *Phys.*

- Rev. D*, vol. 111, no. 8, p. 084064, 2025.
- [47] R. Abbott *et al.*, “GWTC-3: Compact Binary Coalescences Observed by LIGO and Virgo during the Second Part of the Third Observing Run,” *Phys. Rev. X*, vol. 13, no. 4, p. 041039, 2023.
- [48] A. Le Tiec and J. Novak, “Theory of gravitational waves,” in *An Overview of Gravitational Waves: Theory, Sources and Detection*, pp. 1–41, World Scientific, 2017.
- [49] D. Liang, Y. Gong, S. Hou, Y. Liu, *et al.*, “Polarizations of gravitational waves in f (r) gravity,” *Physical Review D*, vol. 95, no. 10, p. 104034, 2017.
- [50] P.-M. Zhang, C. Duval, G. Gibbons, and P. Horvathy, “Velocity memory effect for polarized gravitational waves,” *Journal of Cosmology and Astroparticle Physics*, vol. 2018, no. 05, p. 030, 2018.
- [51] S. Hou, Y. Gong, and Y. Liu, “Polarizations of gravitational waves in horndeski theory,” *The European Physical Journal C*, vol. 78, no. 5, p. 378, 2018.
- [52] M. Mewes, “Signals for lorentz violation in gravitational waves,” *Physical Review D*, vol. 99, no. 10, p. 104062, 2019.
- [53] D. Liang, R. Xu, X. Lu, and L. Shao, “Polarizations of gravitational waves in the bumblebee gravity model,” *Physical Review D*, vol. 106, no. 12, p. 124019, 2022.
- [54] B. P. e. a. L. S. C. Abbott and V. Collaboration), “Tests of general relativity with gw150914,” *Phys. Rev. Lett.*, vol. 116, p. 221101, 2016.
- [55] B. P. e. a. Abbott, “Gw170817: Observation of gravitational waves from a binary neutron star inspiral,” *Phys. Rev. Lett.*, vol. 119, p. 161101, 2017.
- [56] V. C. Abbott, R. et al. (LIGO Scientific Collaboration, “Tests of general relativity with binary black holes from the ligo–virgo catalog gwtc-3,” *Phys. Rev. D*, vol. 105, p. 042003, 2022.
- [57] A. A. Araújo Filho and J. A. A. S. Reis, “How does geometry affect quantum gases?,” *International Journal of Modern Physics A*, vol. 37, no. 11n12, p. 2250071, 2022.
- [58] A. A. Araújo Filho, *Thermal aspects of field theories*. Amazon. com, 2022.
- [59] J. Furtado, H. Hassanabadi, J. Reis, *et al.*, “Thermal analysis of photon-like particles in rainbow gravity,” *arXiv preprint arXiv:2305.08587*, 2023.
- [60] R. Oliveira *et al.*, “Thermodynamic properties of neutral dirac particles in the presence of an electromagnetic field,” *The European Physical Journal Plus*, vol. 135, no. 1, pp. 1–10, 2020.
- [61] A. A. Araújo Filho, “Thermodynamics of massless particles in curved spacetime,” *International Journal of Geometric Methods in Modern Physics*, vol. 20, no. 13, p. 2350226, 2023.